

# Numerical investigation of the quantum fluctuations of optical fields transmitted through an atomic medium

A. Lezama,<sup>1</sup> P. Valente,<sup>2</sup> H. Failache,<sup>1</sup> M. Martinelli,<sup>2</sup> and P. Nussenzveig<sup>2</sup>

<sup>1</sup>*Facultad de Ingeniería, Instituto de Física, Casilla de correo 30, 11000, Montevideo, Uruguay*

<sup>2</sup>*Instituto de Física, Universidade de São Paulo, Caixa Postal 66318, 05315-970, São Paulo, São Paulo, Brazil*

(Received 2 October 2007; published 11 January 2008)

We have numerically solved the Heisenberg-Langevin equations describing the propagation of quantized fields through an optically thick sample of atoms. Two orthogonal polarization components are considered for the field, and the complete Zeeman sublevel structure of the atomic transition is taken into account. Quantum fluctuations of atomic operators are included through appropriate Langevin forces. We have considered an incident field in a linearly polarized coherent state (driving field) and vacuum in the perpendicular polarization and calculated the noise spectra of the amplitude and phase quadratures of the output field for two orthogonal polarizations. We analyze different configurations depending on the total angular momentum of the ground and excited atomic states. We examine the generation of squeezing for the driving-field polarization component and vacuum squeezing of the orthogonal polarization. Entanglement of orthogonally polarized modes is predicted. Noise spectral features specific to (Zeeman) multilevel configurations are identified.

DOI: [10.1103/PhysRevA.77.013806](https://doi.org/10.1103/PhysRevA.77.013806)

PACS number(s): 42.50.Ct, 42.50.Dv, 42.50.Gy, 03.67.Mn

## I. INTRODUCTION

The preparation of optical fields in states with purely quantum-mechanical properties is the key ingredient of quantum optics and the essential requirement for their use in quantum-information processing. Light fields presenting squeezing are well-known examples of nonclassical states for which numerous applications have been suggested and demonstrated. Entanglement of a two-mode field is another important example of a purely quantum-mechanical resource which lies at the basis of a large number of quantum-information procedures such as Einstein-Podolsky-Rosen (EPR) pair production, teleportation, and quantum cryptography [1]. For two degenerate field modes, considered as continuous-variable systems, squeezing and entanglement are related concepts. Squeezing in one mode leads to entanglement between two modes obtained by a linear optical transformation, as implemented by a beam splitter [2,3].

Ever since the first proposals for light squeezing, atomic systems have attracted considerable attention owing to the large nonlinearities associated with resonant transitions. Indeed, the first successful demonstration of squeezing used nondegenerate four-wave mixing in sodium atoms [4] contained in an optical cavity. Several subsequent experiments [5,6] also used atomic samples contained in optical cavities. In these experiments, the highly nonlinear interaction between the atoms and the cavity mode plays an essential role in the generation of squeezing.

Following the early work, most present-day experiments on the generation of nonclassical fields with atomic samples involve the use of optical cavities and require rather complicated experimental setups [7–9]. However, in view of applications, the use of single-path schemes for the generation of nonclassical light fields could be of considerable practical interest. In this paper, we are concerned with the modification of quantum fluctuations of a single monochromatic light beam interacting with an atomic medium on a single path. This possibility is already implicit in the pioneering work by

Walls and Zoller [10] and Mandel [11] predicting reduced quantum fluctuations in the light emitted by a resonantly driven two-level atom. The spectral distribution of the quadrature fluctuations of light emitted by a driven two-level atom was first calculated in [12]. The generalization of this study to an extended atomic sample was carried out by Heidmann *et al.* [13], who considered the fluctuations in the field emitted in the forward direction by a thin layer of atoms at rest, driven by a normally incident laser beam. At low laser intensities, squeezing is predicted for the low-frequency components of the in-phase quadrature. For saturating intensities, squeezing occurs for noise frequencies around the generalized Rabi frequency  $\Omega = (\Delta^2 + \Omega_0^2)^{1/2}$ , where  $\Delta$  is the atom-laser detuning, and  $\Omega_0$  the incident-field resonant Rabi frequency. The calculation of the fluctuation spectra of light traversing a thick two-level atom medium was presented by Ho *et al.* [14]. Single-path squeezing was observed using sodium [15] and ytterbium [16]. Quite recently, intensity-intensity quantum correlations (sub-shot-noise intensity-difference noise) were observed in nondegenerate forward four-wave mixing in rubidium vapor [17].

The initial work on squeezing through light-atom interaction considered ideal two-level transitions and a single-mode optical field. A more realistic approach requires the consideration of multimode light fields (including different polarizations) and multilevel atoms. Three-level atoms interacting with two fields ( $\Lambda$  systems) have been analyzed. Such systems are of considerable interest owing to the possibility of large nonlinearities in association with electromagnetically induced transparency (EIT). Phase-noise squeezing was predicted for a  $\Lambda$  system in which one of the fields was classical, for a cavity-contained atomic system [18], and for single-path propagation through an ensemble of motionless atoms [19].

An interesting issue of the multimode field interaction with an atomic sample is the possibility of achieving polarization squeezing, which is signaled by squeezing of the vacuum field with orthogonal polarization relative to the in-

cident field. Polarization squeezing with cold atoms inside an optical cavity was demonstrated by Josse and co-workers [8,20]. Polarization squeezing is intimately related to the observation of continuous-variable entanglement between two field modes [9,21–23].

Recently, a renewal of attention in the fluctuations of light transmitted through an atomic sample was motivated by the prediction that vacuum-field squeezing could be achieved on a single path as a consequence of polarization self-rotation (PSR) [24]. An experimental observation of squeezing via PSR was reported [25], using a room-temperature rubidium cell. This result could not be reproduced by other groups, in spite of the methodical exploration of the relevant experimental parameter space [26]. It is argued by Hsu and co-workers [26] that excess noise, preventing the observation of squeezing via PSR, originates from the quantum atomic fluctuations not explicitly included in the original theoretical proposal [24]. This argument is supported by a simplified four-level system model [20], for which the noise arising from atomic quantum fluctuations dominates over the semi-classical squeezing terms, under the conditions corresponding to the experiments. However, PSR squeezing is not excluded for cold atom samples in the regime of large intensities and optical detunings.

The noise properties of light fields interacting with atom samples on a single path have been experimentally investigated under conditions of EIT. Large correlations and anticorrelations were observed between the two fields at the Raman resonance condition between the two ground-state hyperfine levels of Rb [27,28]. The change in sign of the correlation is determined by the light intensity. Noise spectra and correlations between two polarization components participating in Hanle-EIT resonance involving Zeeman sublevels of the Rb ground state were observed [29]. These studies were carried out using diode lasers, known to possess large excess phase noise. A qualitative agreement between these experiments and theory could be reached by considering a classical field with random phase diffusion.

All theoretical models considered so far in connection with the analysis of light fluctuations interacting with an atomic sample are based on several simplifications. Single-mode approaches ignore the light polarization orthogonal to the incident field, through which vacuum fluctuations enter the atomic system. Such fluctuations interact with the incident field, provided the sample possesses or acquires some anisotropy through interaction with light. Multimode models also rely on simplifying assumptions. Sometimes one of the incident fields is taken as classical [18]. The transverse spatial structure of the field is generally not considered [30]. In most cases, quantum fluctuations of the atomic operators are ignored. Even when a full quantum treatment was used, the atomic level structure considered was assumed to be an ideal three- or four-level system. In most studies, the effect of propagation through an optically thick sample is not examined. The effect of the atomic velocity distribution and that of nearby atomic levels within the hyperfine structure is usually neglected.

It is the purpose of this work to investigate the quantum noise in fields transmitted through a homogeneous atomic sample when the full Zeeman degeneracy of the ground and

excited atomic levels is taken into account. We consider a light field incident on the atomic sample with a well-defined polarization and take into account the incoming vacuum-field fluctuations with orthogonal polarization. We calculate the field fluctuation noise spectrum after propagation through the medium for arbitrary polarization and field quadrature angle, fully taking into account the influence of the quantum fluctuations of the atomic medium. Depending on the choice of the ground- and excited-level angular momenta ( $F_g$  and  $F_e$ , respectively) and the field polarization, several configurations can be analyzed. A two-level system is obtained for a  $F_g=0 \rightarrow F_e=1$  transition. An open  $\Lambda$  system is obtained for a  $F_g=1 \rightarrow F_e=0$  transition, if the incident field is linearly polarized and the two circular polarization components are considered. The four-level system studied in [20] corresponds to an  $F_g=1/2 \rightarrow F_e=1/2$  transition, with linear field polarization. In addition to those schemes previously explored, our calculation allows us to address other configurations, such as  $F_g \neq 0 \rightarrow F_e=F_g+1$ , for which no full quantum treatment was previously reported in spite of the prediction of PSR squeezing in this system [24]. Our calculation considers a one-dimensional propagation (along the  $z$  axis) through a spatially homogeneous atomic sample considered as a continuous medium [31]. We begin by assuming that the atoms are at rest. Next, we briefly address the effect of a thermal atomic velocity distribution. Propagation effects on quantum fluctuations for a thick medium, of length  $L$ , are included in the calculation, although the depletion of the incident-field mean value is ignored for simplicity. Thus, our results can be directly applied to situations in which absorption of the carrier frequency component of the field can be neglected (saturating field intensities or large atom-field detunings).

Our calculation confirms the prediction of quadrature squeezing under several conditions and indicates that squeezing by PSR can take place for  $F_g=1/2 \rightarrow F_e=1/2$  transitions, and for  $F_g > 0 \rightarrow F_e=F_g+1$  transitions as well. The rather complex structure of the noise spectrum for thick optical media is illustrated and additional features in the noise spectrum specific of the multilevel Zeeman structure are presented.

The paper is organized as follows. In the next section, the main lines of our theoretical model and noise spectrum calculation are presented. In Sec. III, we present and discuss the noise spectra corresponding to different level schemes. Concluding remarks are made in Sec. IV.

## II. MODEL

The problem that we address in this paper is schematically presented in Fig. 1. A laser beam traverses an optically thick atomic sample. The polarization of the incident driving field is defined by appropriate polarization optics. After the sample, the field is decomposed into two chosen orthogonal polarizations. The quadrature noise on both polarization components is analyzed by homodyne detection [32].

Our theoretical approach follows closely the method used by Dantan and co-workers [33] for the study of the propagation of light fluctuations through an ensemble of three-level

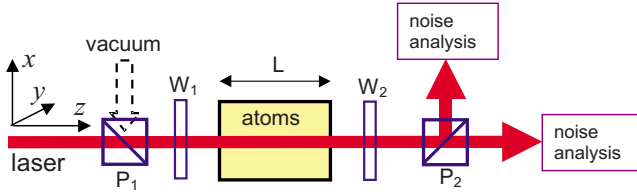


FIG. 1. (Color online) Scheme of the physical situation theoretically addressed in this paper ( $P_1, P_2$ , polarizers;  $W_1, W_2$ , wave plates). The driving field polarization is imposed by  $P_1$  and  $W_1$ , while  $W_2$  and  $P_2$  achieve the decomposition of the transmitted field into orthogonal polarization components. The noise analysis is made by homodyne detection. In the calculations, we have chosen linear  $x$  polarization for the driving field and analyzed fluctuations for polarizations  $x$  and  $y$ .

atoms in a  $\Lambda$  configuration. We consider two levels with Zeeman sublevels: a ground state  $g$ , of total angular momentum  $F_g$  and zero energy, and an excited state  $e$ , of angular momentum  $F_e$  and energy  $\hbar\omega_0$ . The total radiative relaxation coefficient of level  $e$  is  $\Gamma$ . We assume that the atoms in the excited state can radiatively decay into the ground state  $g$  at a rate  $b\Gamma$ , where  $b$  is a branching ratio coefficient that depends on the specific atomic transition ( $0 \leq b \leq 1$ ). For a closed (cycling) transition,  $b=1$ . When the transition is open ( $b < 1$ ), excited atoms can decay back into level  $g$  or into levels external to the two-level system. The atoms are in the presence of a magnetic field  $\mathcal{B}$  directed along the light propagation axis  $z$ . In order to simulate the effect of a finite interaction time of the atoms with the light, we introduce an overall phenomenological decay constant  $\gamma$  ( $\gamma \ll \Gamma$ ), which is compensated, in the steady state, by the arrival of fresh atoms in the ground state. We initially analyze a homogeneous ensemble of atoms at rest, leaving the effect of the atomic velocity distribution for subsequent consideration.

Incident upon the atoms is a light field described in the Heisenberg picture by the operator

$$\begin{aligned} \vec{E}(z, t) = & \xi(a_1 e^{i(kz - \omega_L t)} \hat{e}_1^* + a_2 e^{i(kz - \omega_L t)} \hat{e}_2^* + a_1^\dagger e^{-i(kz - \omega_L t)} \hat{e}_1 \\ & + a_2^\dagger e^{-i(kz - \omega_L t)} \hat{e}_2), \end{aligned} \quad (1)$$

where  $\hat{e}_1$  and  $\hat{e}_2$  are two orthogonal (complex) polarization unit vectors and  $a_1, a_2, a_1^\dagger$ , and  $a_2^\dagger$  are the slowly varying field operators obeying the commutation rules

$$[a_\kappa(z, t), a_\lambda(z', t')] = 0$$

and

$$[a_\kappa(z, t), a_\lambda^\dagger(z', t')] = (L/c) \delta_{\kappa\lambda} \delta(t - t' - \frac{z-z'}{c}).$$

The quantization length  $L$  is chosen as the atomic medium length and  $c$  is the speed of light in vacuum.  $\xi = \sqrt{\hbar\omega_L/2\epsilon_0SL}$  is the single-photon field amplitude (where  $S$  is the mode cross section).

The atomic operators in the Heisenberg representation for an atom  $j$  at position  $z_j$  are  $\rho_{\mu\nu}^j(t) = |\nu\rangle\langle\mu|_j$  where  $|\mu\rangle$  and  $|\nu\rangle$  designate Zeeman substates. We introduce the slowly varying atomic operators  $\sigma_{\mu\nu}^j(z_j, t) = U\rho_{\mu\nu}^j(t)U^\dagger$ , where  $U = P_g^j e^{i(kz_j - \omega_L t)} + P_e^j$  is a unitary transformation.  $P_g^j$  and  $P_e^j$  are

the projectors on ground- and excited-state manifolds, respectively. Following [33], we define continuous local operators (at position  $z$ ) by averaging over a slice of the atomic medium of length  $\Delta z$ :

$$\sigma_{\mu\nu}(z, t) = \lim_{\Delta z \rightarrow 0} \frac{L}{N\Delta z} \sum_{z \leq z_j \leq z + \Delta z} \sigma_{\mu\nu}^j(z_j, t), \quad (2)$$

where  $L$  is the total length of the atomic medium and  $N$  the number of atoms.

The atomic Hamiltonian is

$$H_A = \frac{N}{L} \int (H_0 + H_B) dz, \quad (3)$$

with  $H_0 = \hbar\omega_0 P_e$  the isolated-atom Hamiltonian and  $H_B = (\beta_g P_g + \beta_e P_e) F_z \mathcal{B}$  the Zeeman coupling with the magnetic field  $\mathcal{B}$ .  $P_e$  and  $P_g$  are the local projectors on the excited and ground manifolds, respectively,  $\beta_g$  and  $\beta_e$  are the ground- and excited-state gyromagnetic factors, and  $F_z$  is the local total angular momentum operator projection along the magnetic-field axis  $z$ .

The atom-field coupling  $H_{\text{int}}$ , in the rotating-wave approximation, is

$$H_{\text{int}} = -\frac{N}{L} \hbar \eta \int [(a_1^\dagger \hat{e}_1 + a_2^\dagger \hat{e}_2) \cdot \vec{Q}_{ge} + \text{H.c.}] dz. \quad (4)$$

Here  $\vec{Q}_{ge} = (\vec{Q}_{eg})^\dagger = P_g \vec{Q} P_e$  is a dimensionless operator related to the atomic electric dipole operator  $\vec{D}$  through  $\vec{D} = \langle g | \vec{D} | e \rangle \vec{Q}$ . The reduced matrix element  $\langle g | \vec{D} | e \rangle$  of the dipole operator between the ground and excited states is taken to be real.  $\eta = \xi \langle g | \vec{D} | e \rangle / \hbar$  is the *reduced* atom-field coupling constant (half the single-photon Rabi frequency). The standard spherical components of the operator  $\vec{Q}_{ge}$  are  $Q_{ge}^q$ , with ( $q = -1, 0, 1$ ). Their matrix elements  $Q_{\mu\nu, ge}^q \equiv \langle \mu | Q_{ge}^q | \nu \rangle$  (where  $\mu$  and  $\nu$  refer to Zeeman substates belonging to the ground and excited manifolds, respectively) are the corresponding Clebsch-Gordan coefficients.

The complete set of atomic operators can be organized into a two-dimensional operator array  $\sigma \equiv \{\sigma_{ij}\}$  whose elements are the individual  $\sigma_{ij}$  operators. After manipulation, one can formally write the Heisenberg-Langevin equations (including relaxation terms) for the atomic operators in the form

$$\begin{aligned} d\sigma/dt = & -i\Delta[P_e, \sigma] - \frac{i}{\hbar}[H_B, \sigma] + i\eta[(a_1 \hat{e}_1^* + a_2 \hat{e}_2^*) \cdot \vec{Q}_{eg} \\ & + \text{H.c.}], \sigma] + b\Gamma(2F_e + 1) \sum_q Q_{ge}^q \sigma Q_{eg}^q - \frac{\Gamma}{2} [P_e, \sigma] \\ & - \gamma(\sigma - \sigma^0) + f, \end{aligned} \quad (5)$$

where  $\Delta = \omega_0 - \omega_L$  is the optical detuning and  $\gamma\sigma_0$  is a pumping term describing the isotropic arrival of fresh atoms in the lower ground state.  $\sigma^0 \equiv \{\sigma_{ij}^0\}$  is chosen such that  $\sigma_{ij}^0 = 0$  for  $i \neq j$ ,  $\sigma_{ij}^0 = 1/(2F_g + 1)$  ( $\mathbb{I}$  is the identity operator) if state  $i$  belongs to the ground level, and  $\sigma_{ij}^0 = 0$  otherwise.  $f \equiv \{f_{ij}\}$  represents the set of Langevin force operators satisfying [33]

$\langle f_{ij}(z, t) f_{kl}^\dagger(z', t') \rangle = (L/N) 2D_{ij,kl} \delta(z-z') \delta(t-t')$ , where  $D_{ij,kl}$  is the corresponding diffusion coefficient.

The field evolution is governed by the Maxwell-Heisenberg equations (in the slowly varying envelope approximation):

$$\left( \frac{\partial}{\partial t} + c \frac{\partial}{\partial z} \right) a_\lambda = iN\eta \hat{e}_\lambda \cdot \sum_{k \in e, l \in g} \vec{Q}_{ge, lk} \sigma_{kl}, \quad (6a)$$

$$\left( \frac{\partial}{\partial t} + c \frac{\partial}{\partial z} \right) a_\lambda^\dagger = -iN\eta \hat{e}_\lambda^* \cdot \sum_{k \in e, l \in g} \sigma_{lk} \vec{Q}_{eg, kl} \quad (6b)$$

with  $\lambda = 1, 2$ .

Equations (5) and (6) form a set of coupled differential equations for the atom-field interaction throughout the atomic sample. We simplify the solution of these equations by assuming that the process is stationary and that the incident-field mean value is undepleted as the atomic medium is traversed,  $\langle a_\lambda(z) \rangle = \langle a_\lambda(0) \rangle = \langle a_\lambda \rangle$ . We proceed by linearizing the field and atom operators  $\sigma_{ij}(z, t) = \langle \sigma_{ij} \rangle + \delta\sigma_{ij}(z, t)$  and  $a_\lambda(z, t) = \langle a_\lambda \rangle + \delta a_\lambda(z, t)$  with  $\langle \delta\sigma_{ij} \rangle = \langle \delta a_\lambda \rangle = 0$ .

The mean value of the atomic operators, given the incident-field mean values, can be obtained by taking the mean value of both sides of Eq. (5). This gives the usual Bloch equations. A numerical solution of these equations was presented in Ref. [34]. We consider next the evolution of the fluctuation operators up to first order. Fourier-transforming the first-order contributions in Eqs. (5) and (6), we get

$$\frac{\partial}{\partial z} \delta a_j(z, \omega) = i \frac{\omega}{c} \delta a_j(z, \omega) + iN \frac{\eta}{c} \hat{e}_j \cdot \sum_{k \in e, l \in g} \vec{Q}_{ge, lk} \delta \sigma_{kl}(z, \omega), \quad (7a)$$

$$\frac{\partial}{\partial z} \delta a_j^\dagger(z, \omega) = i \frac{\omega}{c} \delta a_j^\dagger(z, \omega) - iN \frac{\eta}{c} \hat{e}_j^* \cdot \sum_{k \in e, l \in g} \delta \sigma_{lk}(z, \omega) \vec{Q}_{eg, kl}, \quad (7b)$$

$$\begin{aligned} f(\omega) = & -i\omega \delta\sigma + i\Delta[P_e, \delta\sigma] + \frac{i}{\hbar} [H_B, \delta\sigma] - i\eta \{ \langle a_1^\dagger \rangle \hat{e}_1 \\ & + \langle a_2^\dagger \rangle \hat{e}_2 \} \cdot \vec{Q}_{ge} + \text{H.c.} \}, \delta\sigma - i\eta \{ (\delta a_1^\dagger \hat{e}_1 + \delta a_2^\dagger \hat{e}_2) \cdot \vec{Q}_{ge} \\ & + \text{H.c.} \}, \langle \sigma \rangle - b\Gamma(2F_e + 1) \left( \sum_q Q_{ge}^q \delta\sigma Q_{eg}^q \right) \\ & + \frac{\Gamma}{2} \{ P_e, \delta\sigma \} + \gamma \delta\sigma, \end{aligned} \quad (8)$$

where  $f(\omega) \equiv \{ f_{ij}(z, \omega) \}$ , with  $\langle f_{ij}(z, \omega) f_{kl}^\dagger(z', \omega') \rangle = (L/N) 2D_{ij,kl} \delta(z-z') \delta(\omega-\omega')$ .

Field fluctuations depend linearly on atomic fluctuations, which in turn are driven by the Langevin force operators. To numerically solve these equations, we adopt a Liouville-space approach [34,35], organizing all operators  $\sigma_{ij}$  into a column vector  $x$ , with  $n=4(F_g+F_e+1)^2$  elements, and the four field operators  $a_1, a_1^\dagger, a_2, a_2^\dagger$  into a four-element

column vector  $A$ . Then, with some manipulation, Eqs. (7) and (8) can be written in the form (we drop the dependence on  $z$  and  $\omega$  for brevity)

$$\frac{\partial \delta A}{\partial z} = i \frac{\omega}{c} \mathbb{I}_4 \delta A + \frac{N\eta}{c} W \delta x, \quad (9)$$

$$-(i\omega \mathbb{I}_n + \mathcal{A}) \delta x = f + \eta V \delta A, \quad (10)$$

where  $\mathbb{I}_n$  is an  $n \times n$  identity matrix,  $W$  is a  $4 \times n$  matrix dependent on the coefficients  $Q_{ij}^q$ ,  $\mathcal{A}$  is an  $n \times n$  matrix corresponding to the atomic evolution (including relaxation terms), and  $V$  is an  $n \times 4$  matrix describing the coupling of the field fluctuations to the atomic operator mean value. By defining  $M \equiv -(i\omega \mathbb{I}_n + \mathcal{A})$ , we can invert Eq. (10) and from Eq. (9) we get

$$\frac{\partial \delta A}{\partial z} = B \delta A + \frac{N\eta}{c} G f, \quad (11)$$

with  $G = WM^{-1}$  a  $4 \times n$  matrix and  $B = [i(\omega/c) \mathbb{I}_4 + (N\eta^2/c)GV]$  a  $4 \times 4$  matrix. A formal solution of Eq. (11) for propagation over a length  $z$  is given by

$$\delta A(z, \omega) = e^{Bz} \left( \delta A(0, \omega) + \frac{N\eta}{c} \int_0^z e^{-Bz'} G f(z', \omega) dz' \right). \quad (12)$$

The power spectra of the field fluctuations after propagation through an atomic medium of thickness  $z$  can be obtained from the matrix  $S(z, \omega)$  related to the field-operator spectral correlation matrix through

$$\langle \delta A(z, \omega) [\delta A(z, \omega')]^\dagger \rangle = \frac{L}{c} S(z, \omega) \delta(\omega - \omega'). \quad (13)$$

Making use of  $\langle f(z, \omega) f^\dagger(z', \omega') \rangle = (L/N) 2D \delta(z-z') \delta(\omega - \omega')$ , where  $D$  is the atomic Langevin force diffusion matrix, and of Eq. (13), one obtains

$$\begin{aligned} S(L, \omega) = & e^{BL} S(0) (e^{BL})^\dagger \\ & + 2 \frac{N\eta^2}{c} e^{BL} \left( \int_0^L e^{-Bz'} G D G^\dagger e^{-B^\dagger z'} dz' \right) e^{B^\dagger L}, \end{aligned} \quad (14)$$

where we have omitted the dependence on  $\omega$  for brevity and taken  $z=L$ .

The term proportional to the identity in  $B$  commutes with all other operators, so we can write

$$S(L, \omega) = e^{KL} S(0) e^{K^\dagger L} + \frac{N\eta^2}{c} e^{KL} \left( \int_0^L e^{-Kz'} J e^{-K^\dagger z'} dz' \right) e^{K^\dagger L}, \quad (15)$$

where  $J = 2GDG^\dagger$  and  $K = (N\eta^2/c)GV$ .

Let  $X'$  be a matrix satisfying

$$-(KX' + X'K^\dagger) = J. \quad (16)$$

Then the integral in Eq. (15) can be evaluated, and we get

$$S(L) = e^{KL}S(0)e^{K^\dagger L} + \frac{N\eta^2}{c}(X' - e^{KL}X'e^{K^\dagger L}). \quad (17)$$

Introducing  $X = (\Gamma X' / L)$  we have:

$$S(L) = e^{C\Gamma GV}S(0)e^{(C\Gamma GV)^\dagger} + C(X - e^{C\Gamma GV}Xe^{(C\Gamma GV)^\dagger}), \quad (18)$$

where  $C = N\eta^2 L / c\Gamma$  is the cooperativity parameter [33,36].

Equation (18) gives the spectral density matrix  $S(L, \omega)$  after the atomic medium, given the incident-field spectral density  $S(0, \omega)$ . The first term on the right-hand side of Eq. (18) represents the semiclassical effect on light fluctuations owing to the mean value of the atomic polarization in response to the mean incident field. Such a term may lead to noise reduction and cross-polarization effects. The second term on the right-hand side of Eq. (18) represents the light noise introduced by the atomic quantum fluctuations via the matrix  $X$ , which is determined by the Langevin force diffusion matrix  $D$  [Eq. (16)]. It always corresponds to *noise increase* (detrimental to squeezing). The calculation of the diffusion matrix  $D$  can be made with the help of the generalized Einstein theorem [37] and the corresponding expressions are given in the Appendix.

In order to be able to calculate noise spectra for arbitrary field quadratures, we introduce the rotated field operator array  $\delta A(\theta) \equiv \{a_1 e^{-i\theta}, a_1^\dagger e^{i\theta}, a_2 e^{-i\theta}, a_2^\dagger e^{i\theta}\}^T$ . It can be immediately calculated as  $\delta A(\theta) = T\delta A$ , where  $T$  is the  $4 \times 4$  matrix with  $e^{-i\theta}$ ,  $e^{i\theta}$ ,  $e^{-i\theta}$ , and  $e^{i\theta}$  along its main diagonal. In a similar way, fluctuations along two arbitrary orthogonal polarization unit vectors  $\hat{e}'_1$  and  $\hat{e}'_2$  can be calculated as  $\delta A'(\theta) = R\delta A(\theta)$ , where  $R$  is the polarization-basis-change matrix. Thus, the spectral density matrix  $S'_\theta(L, \omega)$  for a given quadrature angle and arbitrary choice of the polarization basis can be evaluated as

$$S'_\theta(L, \omega) = TRS(L, \omega)R^\dagger T^\dagger. \quad (19)$$

The noise spectrum  $s'_{j\theta}$  for the quadrature angle  $\theta$  of the field with polarization  $\hat{e}'_j$  ( $j=1, 2$ ), as can be measured by homodyne detection, can be evaluated from the matrix elements  $S'_{\theta\mu\nu}$  of  $S'_\theta(L, \omega)$ . Dropping, for brevity, the  $L$  and  $\omega$  dependence, we have

$$s'_{1\theta} = S'_{\theta 11} + S'_{\theta 12} + S'_{\theta 21} + S'_{\theta 22}, \quad (20a)$$

$$s'_{2\theta} = S'_{\theta 33} + S'_{\theta 34} + S'_{\theta 43} + S'_{\theta 44}. \quad (20b)$$

Other matrix elements of  $S'_\theta$  not appearing in Eqs. (20a) and (20b) are related to the field correlations between the two polarizations.

### Velocity distribution

So far we have considered a homogeneous sample of atoms at rest. We will generalize now our calculation to a sample of moving atoms with velocity  $v_z$  in the direction of the light propagation axis. The velocity distribution is  $\mathcal{W}(v_z)$ , obeying  $\int_{-\infty}^{+\infty} \mathcal{W}(v_z) dv_z = 1$ . Then Eq. (11) becomes:

$$\frac{\partial[\delta A(z, \omega)]}{\partial z} = B' \delta A + \frac{N\eta}{c} \int_{-\infty}^{+\infty} \mathcal{W}(v_z) G(v_z) f_{v_z} dv_z, \quad (21)$$

with

$$B' = i\frac{\omega}{c}\mathbb{I}_4 + \frac{N\eta^2}{c} \int_{-\infty}^{+\infty} \mathcal{W}(v_z) G(v_z) V(v_z) dv_z, \quad (22)$$

$$G(v_z) = WM(v_z)^{-1}, \quad (23)$$

$$M(v_z) \equiv -i\omega\mathbb{I}_n + \mathcal{A}(v_z). \quad (24)$$

$\mathcal{A}(v_z)$  depends on  $v_z$  through the velocity-dependent detuning  $\Delta = \omega_0 - \omega_L - kv_z$  [see Eq. (5)] and  $V(v_z)$  depends on  $v_z$  through the mean values  $\langle x(v_z) \rangle$ .

After formal integration of Eq. (21) one has

$$\delta A(z, \omega) = e^{B'z} \left( \delta A(0, \omega) + \frac{N\eta}{c} \int_0^z e^{-B'z'} \times \int_{-\infty}^{+\infty} \mathcal{W}(v_z) G(v_z) f(v_z, z', \omega) dv_z dz' \right). \quad (25)$$

Since the Langevin forces for atoms with different velocities are uncorrelated, we impose

$$\langle f(z, v_z, \omega) f^\dagger(z', v'_z, \omega') \rangle = \frac{L}{N\mathcal{W}(v_z)} 2D \delta(z - z') \delta(\omega - \omega') \times \delta(v_z - v'_z). \quad (26)$$

Using Eqs. (25) and (26) one can obtain the spectral density matrix for the output field as

$$S(L) = e^{K'L}S(0)e^{K'^\dagger L} + \frac{N\eta^2}{c} e^{K'L} \left( \int_0^L e^{-K'z'} J' e^{-K'^\dagger z'} dz' \right) e^{K'^\dagger L}, \quad (27)$$

with

$$K'L = C\Gamma \int_{-\infty}^{+\infty} \mathcal{W}(v_z) G(v_z) V(v_z) dv_z \quad (28)$$

and

$$J' = \int_{-\infty}^{+\infty} \mathcal{W}(v_z) G(v_z) D G(v_z)^\dagger dv_z. \quad (29)$$

The expression for the spectral density matrix given in Eq. (27) represents a generalization of Eq. (15) that can be evaluated by the same method. The integrals in Eqs. (28) and (29) can be evaluated numerically, given the velocity distribution  $\mathcal{W}(v_z)$ .

### III. CALCULATED NOISE SPECTRA

The model developed in Sec. II allows us to calculate the spectral density of the fields transmitted through a homogeneous atomic sample of thickness  $L$  and total number of atoms  $N$  under a wide range of conditions, i.e., arbitrary

choices of the atomic levels' angular momenta, driving-field polarization, and incident field mean intensity. In addition, the model allows the arbitrary choice of the branching ratio  $b$  and the longitudinal magnetic field  $B$ . However, in this paper we will restrict ourselves to considering a reduced number of parameters. No magnetic field is considered. In addition, the branching ratio  $b$  is taken as one which means that no transition to states external to the two-level system are allowed. This assumption may not necessarily correspond to actual observable atomic transitions. Although the detailed study of the role of the branching  $b$  is beyond the scope of this work, one should notice that some choices of  $F_g$  and  $F_e$  effectively describe open systems since there are trapping (dark) states not coupled to the applied field. The driving field polarization ( $\hat{e}_1$ ) is chosen to be linear along axis  $x$ , which means that vacuum enters the system with  $y$  polarization ( $\hat{e}_2$ ). The  $x$ -polarized driving field is assumed to be in a coherent state  $|\alpha\rangle$ . The corresponding reduced Rabi frequency (independent of polarization and atomic dipole orientation) is  $\Omega_r = 2\alpha\eta$ , taken real. Under these conditions, the incident (white noise) spectral density matrix is [35]

$$S(0, \omega) = \begin{pmatrix} 1 & 0 & 0 & 0 \\ 0 & 0 & 0 & 0 \\ 0 & 0 & 1 & 0 \\ 0 & 0 & 0 & 0 \end{pmatrix}, \quad (30)$$

in units for which the standard quantum noise limit corresponds to 1.

We have analyzed the output-field fluctuations for the same set of orthogonal polarizations ( $x$  and  $y$ ) used for the incident field [ $R = \mathbb{I}_4$  in Eq. (19)]. Noise spectra for a different choice of the polarization basis can be easily obtained using the appropriate matrix  $R$ . We have calculated the spectra for both the amplitude quadrature ( $\theta=0$ ) and the phase quadrature ( $\theta=\pi/2$ ). In all calculations, the relaxation rate  $\gamma$  was taken as  $\gamma=0.01\Gamma$ , a realistic figure for experiments using alkali-metal-atom  $D$  lines. In the following, we analyze different level schemes depending on the angular momentum of the ground and excited states. We begin by considering the case of a homogenous sample of atoms at rest (cold atom sample). The effect of atomic motion is discussed at the end of this section.

#### A. $F_g=0 \rightarrow F_e=1$

Choosing the quantization axis in the direction ( $x$ ) of the linear polarization of the applied field, this case reduces to a pure two-level system in which the field couples the Zeeman sublevels  $|F_g=0, m_g=0\rangle$  and  $|F_e=1, m_e=0\rangle$ . The  $y$  polarization, along which vacuum is entering the atomic system, is totally uncoupled to the driven transition. As a consequence, no change takes place for the  $y$ -polarization mode and this field emerges from the sample in the vacuum state.

The results of our model are in agreement with previous work on quantum fluctuations and squeezing for pure two-level atoms [12–14]. Figure 2 presents the noise spectra obtained for both quadratures in the case of resonant atomic excitation ( $\Delta=0$ ) for a rather thin sample ( $C=1$ ), for differ-

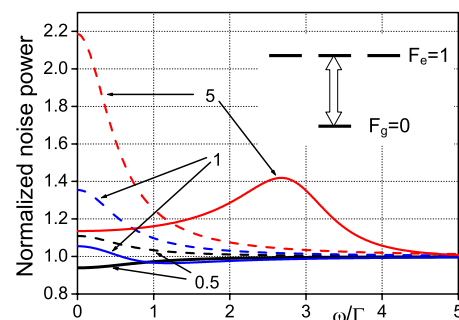


FIG. 2. (Color online) Transition  $F_g=0 \rightarrow F_e=1$ . (Inset: the level scheme is shown using  $x$  as the quantization axis; hollow arrow shows the driving field.) Noise spectra normalized to the standard quantum noise limit of the amplitude (solid) and phase (dashed) quadratures of the transmitted field with the same linear polarization as the driving field, at zero detuning. The different values of the reduced Rabi frequency  $\Omega_r$  (in units of  $\Gamma$ ) are indicated ( $C=1$ ,  $\gamma=0.01\Gamma$ ).

ent values of the reduced Rabi frequency  $\Omega_r$ . Excess noise, with maximum value at zero frequency, is obtained for the phase quadrature for all field intensities. The amplitude quadrature presents squeezing centered at zero frequency for small light-field amplitude ( $\Omega_r \lesssim 0.5\Gamma$ ). As the Rabi frequency increases, the maximum squeezing shifts to increasing nonzero frequencies and disappears as  $\Omega_r > \Gamma$ . For large  $\Omega_r$ , the intensity fluctuations present an excess noise peak centered at the *actual* Rabi frequency  $\Omega_0$ . Notice that, since  $\Omega_r$  is the reduced Rabi frequency, the actual Rabi frequency associated with the specific two-level transition is  $\Omega_0 = (Q_{00,ge}^0)\Omega_r = (1/\sqrt{3})\Omega_r$ . As discussed in [13], amplitude squeezing occurs in this case only in the limit of an optically thin medium, where the amount of squeezing is linearly dependent on  $C$ . However, at zero detuning, the mean field absorption, which is not taken into account in our treatment, is considerable and also linearly dependent on  $C$ . Consequently, absorption of the incident field should prevent the observation of squeezing in this regime. To avoid the effect of field absorption, one should consider situations in which the generalized Rabi frequency  $\Omega = (\Delta^2 + \Omega_0^2)^{1/2}$  is large. This case corresponds to well-resolved levels in the dressed-atom picture [38]. Noise spectra calculated for  $\Delta = \Omega_r = 10\Gamma$  are presented in Fig. 3, for different values of the cooperativity parameter.  $C=1$  corresponds to a thin atomic medium. The noise spectrum is essentially dominated by a peak occurring at  $\omega = \Omega$ . Squeezing occurs for the phase quadrature and, correspondingly, excess noise is present in the amplitude quadrature. The observed squeezing is due to four-wave mixing between the mean field at the carrier frequency  $\omega_L$  and the noise sidebands at frequencies  $\omega_L \pm \omega$  [14]. In the dressed-atom picture of the atoms driven by the incident mean field, a double  $\Lambda$  scheme occurs, involving the absorption (emission) of two driving-field photons and the emission (absorption) of a photon from each of the two sidebands (see inset in Fig. 4). This mechanism results in the buildup of correlations between the two sideband fluctuations, leading to quadrature squeezing [32]. This process is fully resonant with the energy levels of the dressed atom when  $\omega = \Omega$ .

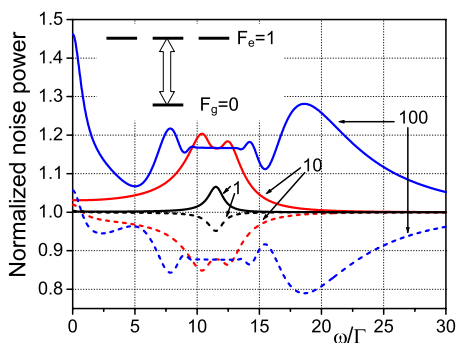


FIG. 3. (Color online) Transition  $F_g=0 \rightarrow F_e=1$ . Noise spectra normalized to the standard quantum noise limit of the amplitude (solid) and phase (dashed) quadratures of the field transmitted with the same linear polarization as the driving field for  $\Delta=10\Gamma=\Omega_r=10\Gamma$ . The different values of the cooperativity parameter  $C$  are indicated ( $\gamma=0.01\Gamma$ ).

As the medium's optical thickness increases, the noise feature around  $\omega=\Omega$  broadens considerably and presents oscillations that are due to the frequency-dependent phase mismatch between the carrier mean field and the noise sidebands [14]. For large  $C$ , broadband squeezing is present. More than 20% squeezing is obtained for  $C=100$ .

We notice from Fig. 3 that, except for the largest value of the cooperativity parameter  $C$ , there is no significant variation of the noise power around zero frequency. This behavior corresponds to closed two-level systems. Open two-level systems show an increase of light fluctuations at low frequency.

The relative effect on the transmitted light fluctuations of the semiclassical atomic response and that of the atomic quantum fluctuations is illustrated in Fig. 4. The total spectrum for the phase quadrature noise and the contributions corresponding to the two terms on the right-hand side of Eq. (18), for  $\Delta=10\Gamma=\Omega_r=10\Gamma$  and  $C=100$ , are shown. As ex-

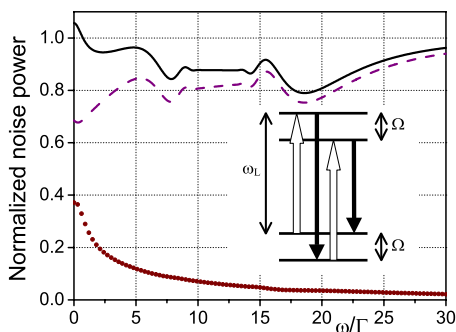


FIG. 4. (Color online) Transition  $F_g=0 \rightarrow F_e=1$ . Solid line: Total noise spectrum normalized to the standard quantum noise limit for the phase quadrature ( $\Delta=\Omega_r=10\Gamma$ ,  $\gamma=0.01\Gamma$ , and  $C=100$ ). Dashed line: Semiclassical contribution [first term on the right-hand side (RHS) of Eq. (18)]. Dotted line: Contribution of the atomic quantum fluctuations [second term on the RHS of Eq. (18)]. Inset: Dressed-atom picture for the four-wave-mixing process responsible for squeezing in two-level atoms. Hollow arrows, laser mean field; solid arrows, noise sidebands.

pected, the squeezing is due only to the semiclassical term contribution. For the chosen parameters, the atomic quantum fluctuations introduce a rather broad and smooth noise increase.

The fact that, for this level scheme, squeezing occurs for one quadrature of the  $x$ -polarized field, while the vacuum fluctuations incident along the  $y$  polarization are unaffected, implies entanglement between two orthogonally polarized modes [39]. This can be explicitly verified by noticing that squeezing of the phase quadrature of field 1 together with vacuum fluctuations in field 2 correspond to

$$\left[ \Delta \left( \frac{a_1 - a_1^\dagger}{i} \right) \right]^2 + \Delta (a_2 + a_2^\dagger)^2 \leq 2. \quad (31)$$

Let us now consider  $a_+=(a_1+a_2)/\sqrt{2}$  and  $a_-=(a_1-a_2)/\sqrt{2}$ , the field operators corresponding to the two orthogonal linear polarizations at  $45^\circ$  with respect to the  $x$  and  $y$  axes. Then the operators  $X_\mu=(a_\mu+a_\mu^\dagger)/\sqrt{2}$  and  $Y_\mu=(a_\mu-a_\mu^\dagger)/i\sqrt{2}$  ( $\mu=+, -$ ) are two pairs of conjugate Hermitian operators satisfying  $[X_\mu, X_\nu]=0$ ,  $[Y_\mu, Y_\nu]=0$ ,  $[X_\mu, Y_\nu]=i\delta_{\mu\nu}$ . For these operators the inequality in Eq. (31) becomes

$$\Delta(Y_+ + Y_-)^2 + \Delta(X_+ - X_-)^2 \leq 2, \quad (32)$$

which is sufficient to demonstrate continuous-variable entanglement of the  $+$  and  $-$  polarization fields [23].

### B. $F_g=1 \rightarrow F_e=0$

Excitation of a transition from a ground state with  $F_g=1$  to an  $F_e=0$  excited state with a linearly ( $x$ ) polarized field corresponds to the coupling of the incident field to an open two-level system. Choosing the quantization axis along  $x$  determines that the incident field is coupled to the  $|F_g=1, m_g=0\rangle$  to  $|F_e=0, m_e=0\rangle$  transition. The excited state can decay into either of the ground-state Zeeman sublevels. Alternatively (in a different basis for the ground-state manifold), the configuration corresponds to the excitation of one branch of a  $\Lambda$  system while the vacuum field is acting on the second branch. A similar situation was studied in [33], in the case of a resonant excitation ( $\Delta=0$ ). Figure 5 shows the noise spectra for both quadratures of the output fields with  $x$  and  $y$  polarizations. The spectra corresponding to the  $x$  polarization are very similar to those obtained for a closed two-level system (Fig. 3), except for the noise increase around zero frequency. Such a low-frequency feature in the noise spectra occurs in open transitions owing to the fluctuations introduced by spontaneous decay out of the two-level system. In addition, an increase in the noise power above the vacuum fluctuations is seen for the  $y$ -polarized field. Both quadratures with this polarization experience the same noise contribution due to spontaneous emission from the excited state. As a consequence of the light shift of the excited state produced by the driving field, the noise for the  $y$  polarization peaks at  $\omega \neq 0$ . In addition to this low-frequency peak, a much smaller local maximum occurs for  $\omega \approx \Omega$ , almost invisible on the scale of Fig. 5.

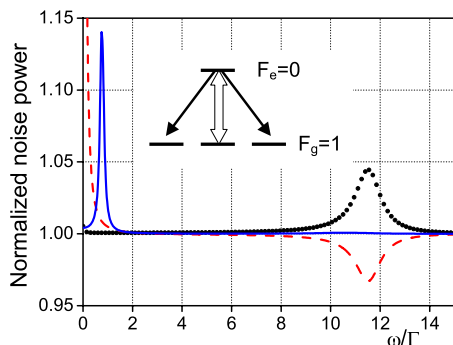


FIG. 5. (Color online) Transition  $F_g=1 \rightarrow F_e=0$  (the level scheme is shown using  $x$  as quantization axis; hollow arrow, driving field; solid arrows, spontaneous emission channels into the  $y$ -polarized mode). Noise spectra normalized to the standard quantum noise limit of the amplitude (dotted) and phase (dashed) quadratures of the transmitted field with the same linear polarization as the driving field. The solid line corresponds to the noise of both quadratures of the output field with polarization orthogonal to the driving field ( $\Delta=\Omega_r=10\Gamma$ ,  $\gamma=0.01\Gamma$ , and  $C=10$ ).

### C. $F_g=1/2 \rightarrow F_e=1/2$

This configuration was analyzed in [20] as a model system for the study of squeezing via PSR. Figure 6 presents the corresponding spectra for resonant excitation ( $\Delta=0$ ). The noise spectra for the driving-field polarization are analogous to those in Fig. 2 for a two-level transition. In fact, for a choice of the quantization axis along  $x$ , the present situation corresponds to two two-level transitions coupled through spontaneous emission. Spontaneous emission is also responsible for the injection of field fluctuations for the  $y$  polarization. Owing to the large symmetry of this configuration, the amplitude noise spectrum for the  $y$  polarization is equal to

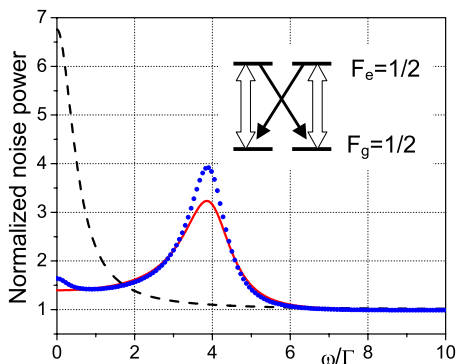


FIG. 6. (Color online) Transition  $F_g=1/2 \rightarrow F_e=1/2$  (the level scheme is shown using  $x$  as quantization axis; hollow arrow, driving field; solid arrows, spontaneous emission channels into the  $y$ -polarized mode). Resonant noise spectra normalized to the standard quantum noise limit of the amplitude (solid) and phase (dashed) quadratures of the transmitted field with the same linear polarization as the driving field. Dotted line: amplitude quadrature noise spectrum of the polarization perpendicular to the driving field, the spectrum of the phase quadrature for this polarization coincides with the dashed line ( $\Delta=0$ ,  $\Omega_r=10\Gamma$ ,  $\gamma=0.01\Gamma$ , and  $C=10$ ).

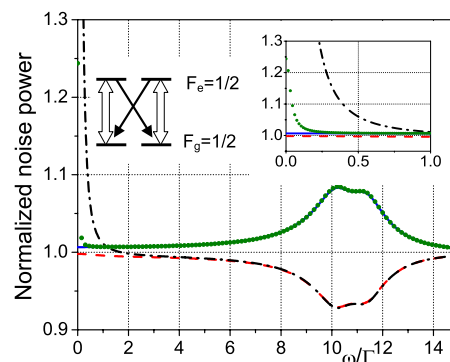


FIG. 7. (Color online) Transition  $F_g=1/2 \rightarrow F_e=1/2$ ,  $\Delta=10\Gamma$ . Noise spectra normalized to the standard quantum noise limit. Amplitude (solid) and phase (dashed) quadratures of the transmitted field with the same linear polarization as the driving field. Amplitude (dash-dotted) and phase (dotted) quadratures of the transmitted field with polarization perpendicular to the driving field. Inset: Expanded low-frequency range ( $\Omega_r=10\Gamma$ ,  $\gamma=0.01\Gamma$ , and  $C=10$ ).

the phase noise spectrum of the  $x$  polarization. The phase noise spectrum for the  $y$  polarization presents enhanced noise if compared to the amplitude quadrature of the  $x$  polarization.

The spectra for a nonresonant excitation ( $\Delta=10\Gamma$ ) are presented in Fig. 7. For  $\omega \geq \Gamma$  the spectra reproduce the features observed for nonresonant excitation of two-level systems (see Fig. 3). Nearly identical noise spectra are obtained for the  $x$ -polarization amplitude (phase) noise and the  $y$ -polarization phase (amplitude) noise. This approximate symmetry is broken for low noise frequencies (see inset in Fig. 7). Squeezing due to PSR occurs in this system for nonzero detuning. In addition, the inequality (31) is verified for  $\omega \sim \Omega$ , giving rise to entanglement.

### D. $F_g=1 \rightarrow F_e=2$

We now consider a transition of the type  $F_g > 0 \rightarrow F_e = F_g + 1$ . For this class of transition, no dark state exists within the ground level. At two-photon Raman resonance between ground-state Zeeman sublevels, coherence resonances occur that correspond to enhanced absorption, that is, electromagnetically induced absorption (EIA) [40,41]. The absorption spectra of a transition of this type driven by a strong classical field were examined in [42]. If a driving field of circular polarization is used, owing to optical pumping, the system approximates a pure two-level system. However, if linear polarization is used for the driving field, while the system is probed along the orthogonal polarization, the absorption spectrum presents a rather complex structure as a result of the different light shifts experienced by the Zeeman sublevels. A simple picture of this effect in terms of the dressed-atom model is presented in [42].

The transmitted-field noise spectra for the transition  $F_g=1 \rightarrow F_e=2$  are presented in Fig. 8 for nonzero detuning ( $\Delta=10\Gamma$ ) and large Rabi frequency ( $\Omega_r=40\Gamma$ ). A thick optical medium is considered ( $C=100$ ). For  $\omega > \Gamma$ , the spectra corresponding to the driving-field polarization are similar to



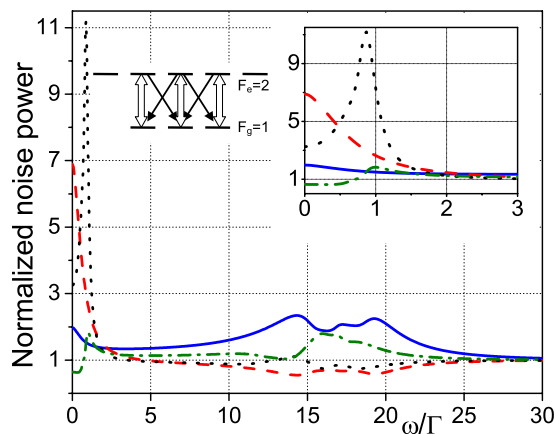


FIG. 8. (Color online) Transition  $F_g=1 \rightarrow F_e=2$  (the level scheme is shown using  $x$  as quantization axis; hollow arrow, driving field; solid arrows, spontaneous emission channels into the  $y$ -polarized mode). Nonresonant noise spectra normalized to the standard quantum noise limit ( $\Delta=10\Gamma$ ). Amplitude (solid) and phase (dashed) quadratures of the transmitted field with the same linear polarization as the driving field. Amplitude (dash-dotted) and phase (dotted) quadratures of the transmitted field with polarization perpendicular to the driving field. Inset: Expanded low-frequency range ( $\Omega_r=40\Gamma$ ,  $\gamma=0.01\Gamma$ , and  $C=100$ ).

the pure two-level spectra shown in Fig. 3. Unlike the pure two-level system, noise is introduced by spontaneous emission into the  $y$ -polarized field. However, PSR squeezing is nevertheless present on the amplitude quadrature for this polarization. In addition, the inequality in Eq. (31) is verified, resulting in entanglement.

At low frequencies ( $\omega \leq \Gamma$ ), the noise spectra present features that are specific to such a multilevel system. Excess noise peaking at  $\omega=0$  occurs for the two quadratures of the driving-field polarization. The orthogonal polarization presents features which are peaked at  $\omega > 0$  owing to the different Zeeman sublevel light shifts [42,43]. Notice the significant squeezing near zero frequency of the phase quadrature.

#### E. Effect of atomic motion

We will now illustrate the effect of atomic motion on the noise spectra for an atomic sample with a Maxwell-Boltzmann velocity distribution. Having in mind the case of rubidium vapor at room temperature, we have used a Doppler width (full width at half maximum)  $\Gamma_{\text{Dopp}}=90\Gamma$ . We consider as an example the  $F_g=1 \rightarrow F_e=2$  transition (same as in Fig. 8).

Figure 9 shows the noise spectra for both field quadratures in the case of a driving field resonant with the zero-velocity atoms and a Rabi frequency  $\Omega_r=40\Gamma$  for  $C=100$ . Notice that, although the average detuning is zero in this case, the noise spectra are reminiscent of those obtained for atoms at rest with nonzero detuning. A local maximum (minimum) is observed for the amplitude (phase) quadrature noise of the driving-field polarization for  $\omega \approx \Omega_0$ . The squeezing of the phase quadrature remains significant ( $\sim 15\%$ ) in spite of the spreading of the field detuning caused

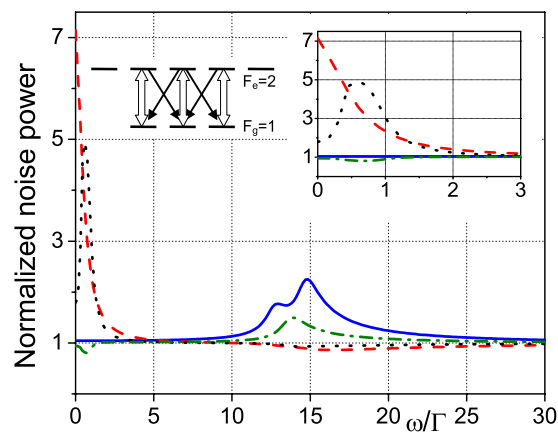


FIG. 9. (Color online) Transition  $F_g=1 \rightarrow F_e=2$ . Noise spectra normalized to the standard quantum noise limit for a Maxwell-Boltzmann atomic velocity distribution and driving field tuned to resonance with zero-velocity atoms. Amplitude (solid) and phase (dashed) quadratures of the transmitted field with the same linear polarization as the driving field. Amplitude (dash-dotted) and phase (dotted) quadratures of the transmitted field with polarization perpendicular to the driving field. Inset: Expanded low-frequency range ( $\Omega_r=40\Gamma$ ,  $\gamma=0.01\Gamma$ ,  $C=100$ , and  $\Gamma_{\text{Dopp}}=90\Gamma$ ).

by the Doppler effect. Notice that the squeezing of the amplitude quadrature noise of the  $y$ -polarized field is not completely suppressed by the velocity distribution, nor are the low-frequency spectral features for both polarizations.

#### IV. CONCLUSIONS

We have developed a theoretical model supporting the numerical calculation of the noise spectra of light traversing an optically thick atomic medium, under a wide range of conditions. The model takes into account the complete Zeeman sublevel structure of the atomic transition and consequently the arbitrary polarization of the light field. In this paper, we have restricted our analysis to the case of a linearly polarized driving field while considering that the Zeeman sublevels are degenerate in the absence of light (zero magnetic field). We have calculated the noise spectra for the amplitude and phase quadratures of the transmitted light with the same and the orthogonal polarization relative to the driving field.

For atoms at rest, as can be produced in magneto-optical traps, the dominant feature of the transmitted-field fluctuation spectra can be traced back to pure two-level atom effects [13]. For nonzero optical detuning, excess noise is introduced in the amplitude quadrature while squeezing occurs for the phase quadrature. The noise variations are maximum for  $\omega=\Omega$ , as a consequence of resonant four-wave mixing of the mean field and noise sidebands with the dressed-atom level structure. The propagation through the optically thick medium results in broadening and oscillatory structure of the noise spectrum owing to phase mismatch between the carrier and the fluctuation sidebands. Up to 30% squeezing occurs for the parameter values used in the simulations, chosen in order to correspond to typical experimental conditions, in-

volving cw lasers and alkali-metal atoms. The figure of  $C = 100$  used in several of the present calculations corresponds to a realistic figure for magneto-optically trapped atom clouds.

In addition to pure two-level atom features, other effects are present as a consequence of the Zeeman sublevel structure. Except when  $F_g=0$ , spontaneous emission introduces noise into the polarization orthogonal to the driving field. Notwithstanding the random field fluctuations caused by spontaneous emission, nonlinear interaction between noise sidebands on both polarizations may result (as in Figs. 7 and 8) in vacuum squeezing for the orthogonal polarization. For the conditions used in our calculations, the noise introduced by the atomic quantum fluctuations does not completely mask the orthogonal polarization vacuum squeezing. Furthermore, for transitions involving multiple Zeeman sublevels, additional structures appear in the noise spectra at low frequency. They come from the different Stark shifts experienced by the Zeeman sublevels in the presence of the driving field. Such low frequency structures are reported here.

The study presented here constitutes a necessary step toward a satisfactory understanding and control of atom-light interaction at the quantum level. This control can be applied to matter-light interfaces for quantum-information purposes, as the entanglement predicted here implies. Further developments may include the influence of nearby transitions as well as that of the spatial structure of the light mode and atomic sample. Pulse propagation effects should also be considered. Such a theoretical approach needs to be complemented with experimental tests, in particular using cold atomic samples. Work in this direction is currently under way.

## APPENDIX: CALCULATION OF THE DIFFUSION COEFFICIENT MATRIX

The Heisenberg-Langevin equation [Eq. (5)] can be written in the form

$$\frac{d\sigma_{ij}}{dt} = \mathcal{D}(\sigma_{ij}) + f_{ij}, \quad (\text{A1a})$$

$$\mathcal{D}(\sigma_{ij}) \equiv \sum_{kl} \mathcal{A}_{ij,kl} \sigma_{kl} + \gamma \sigma_{ij}^0, \quad (\text{A1b})$$

where  $\mathcal{A} \equiv \{\mathcal{A}_{ij,kl}\}$  is the matrix appearing in Eq. (10). The Langevin forces obey:  $\langle f_{ij}(z,t) f_{kl}^\dagger(z',t') \rangle = (L/N) 2D_{ij,kl} \delta(z-z') \delta(t-t')$ . The diffusion matrix  $D = \{D_{ij,kl}\}$  can be calculated with the help of the generalized Einstein relation [37,38]

$$2D_{ij,kl} = \langle \mathcal{D}(\sigma_{ij} \sigma_{kl}^\dagger) - \mathcal{D}(\sigma_{ij}) \sigma_{kl}^\dagger - \sigma_{ij} \mathcal{D}(\sigma_{kl}^\dagger) \rangle. \quad (\text{A2})$$

From Eq. (A1b), by making use of  $\sigma_{ij}^\dagger \sigma_{kl} \equiv |i\rangle\langle j| |l\rangle\langle k| = \sigma_{ik}^\dagger \delta_{jl}$  and  $\mathcal{A}_{ij,mm} = \mathcal{A}_{ji,mm}^*$ , we get

$$\langle \mathcal{D}(\sigma_{ij} \sigma_{kl}^\dagger) \rangle = 0,$$

$$\langle \mathcal{D}(\sigma_{ij}) \sigma_{kl}^\dagger \rangle = \sum_m \mathcal{A}_{ij,km} \langle \sigma_{lm} \rangle + \gamma \sigma_{ij}^0 \langle \sigma_{lk} \rangle,$$

$$\langle \sigma_{ij} \mathcal{D}(\sigma_{kl}^\dagger) \rangle = \sum_m \mathcal{A}_{lk,mi} \langle \sigma_{mj} \rangle + \gamma \langle \sigma_{ij} \rangle \sigma_{lk}^0. \quad (\text{A3})$$

The first of Eqs. (A3) results from the stationarity of the system. The mean values  $\langle \sigma_{ij} \rangle$  are obtained from the steady-state solution of Eq. (A1a).

- 
- [1] M. Terhal, M. Wolf, and A. Doherty, *Phys. Today* **56** (4), 46 (2003).  
 [2] N. Bohr, *Phys. Rev.* **48**, 696 (1935); see footnote on p. 696.  
 [3] M. S. Kim, W. Son, V. Bužek, and P. L. Knight, *Phys. Rev. A* **65**, 032323 (2002).  
 [4] R. E. Slusher, L. W. Hollberg, B. Yurke, J. C. Mertz, and J. F. Valley, *Phys. Rev. Lett.* **55**, 2409 (1985).  
 [5] M. G. Raizen, L. A. Orozco, M. Xiao, T. L. Boyd, and H. J. Kimble, *Phys. Rev. Lett.* **59**, 198 (1987).  
 [6] D. M. Hope, H.-A. Bachor, P. J. Manson, D. E. McClelland, and P. T. H. Fisk, *Phys. Rev. A* **46**, R1181 (1992).  
 [7] A. Lambrecht, T. Coudreau, A. Steinberg, and E. Giacobino, *Europhys. Lett.* **36**, 93 (1996).  
 [8] V. Josse, A. Dantan, L. Vernac, A. Bramati, M. Pinard, and E. Giacobino, *Phys. Rev. Lett.* **91**, 103601 (2003).  
 [9] V. Josse, A. Dantan, A. Bramati, M. Pinard, and E. Giacobino, *Phys. Rev. Lett.* **92**, 123601 (2004).  
 [10] D. F. Walls and P. Zoller, *Phys. Rev. Lett.* **47**, 709 (1981).  
 [11] L. Mandel, *Phys. Rev. Lett.* **49**, 136 (1982).  
 [12] M. Collett, D. Walls, and P. Zoller, *Opt. Commun.* **52**, 145 (1984).  
 [13] A. Heidmann and S. Reynaud, *J. Phys.* **46**, 1937 (1985).  
 [14] S.-T. Ho, P. Kumar, and J. H. Shapiro, *Phys. Rev. A* **35**, 3982 (1987).  
 [15] S. Ho, N. Wong, and J. Shapiro, *Opt. Lett.* **16**, 840 (1991).  
 [16] Z. H. Lu, S. Bali, and J. E. Thomas, *Phys. Rev. Lett.* **81**, 3635 (1998).  
 [17] C. McCormick, V. Boyer, E. Arimondo, and P. Lett, *Opt. Lett.* **32**, 178 (2007).  
 [18] M. Fleischhauer, U. Rathe, and M. O. Scully, *Phys. Rev. A* **46**, 5856 (1992).  
 [19] U. W. Rathe, M. Fleischhauer, and M. O. Scully, *Phys. Rev. A* **54**, 3691 (1996).  
 [20] V. Josse, A. Dantan, A. Bramati, M. Pinard, and E. Giacobino, *J. Opt. B: Quantum Semiclass. Opt.* **5**, S513 (2003).  
 [21] A. Dantan, J. Cviklinski, E. Giacobino, and M. Pinard, *Phys. Rev. Lett.* **97**, 023605 (2006).  
 [22] S. Pielawa, G. Morigi, D. Vitali, and L. Davidovich, *Phys. Rev. Lett.* **98**, 240401 (2007).  
 [23] L.-M. Duan, G. Giedke, J. I. Cirac, and P. Zoller, *Phys. Rev. Lett.* **84**, 2722 (2000).  
 [24] A. B. Matsko, I. Novikova, G. R. Welch, D. Budker, D. F. Kimball, and S. M. Rochester, *Phys. Rev. A* **66**, 043815 (2002).  
 [25] J. Ries, B. Brezger, and A. I. Lvovsky, *Phys. Rev. A* **68**, 025801 (2003).

- [26] M. T. L. Hsu *et al.*, Phys. Rev. A **73**, 023806 (2006).
- [27] C. L. Garrido Alzar, L. S. Cruz, J. G. Aguirre Gómez, M. França Santos, and P. Nussenzveig, Europhys. Lett. **61**, 485 (2003).
- [28] L. Cruz, D. Felinto, J. Aguirre Gómez, M. Martinelli, P. Valente, A. Lezama, and P. Nussenzveig, Eur. Phys. J. D **41**, 531 (2007).
- [29] M. Martinelli, P. Valente, H. Failache, D. Felinto, L. S. Cruz, P. Nussenzveig, and A. Lezama, Phys. Rev. A **69**, 043809 (2004).
- [30] A. Lambrecht, J. Courty, and S. Reynaud, J. Phys. II **6**, 1133 (1996).
- [31] M. Fleischhauer and T. Richter, Phys. Rev. A **51**, 2430 (1995).
- [32] H.-A. Bachor, *A Guide to Experiments in Quantum Optics* (Wiley-VCH, Weinheim, 1998).
- [33] A. Dantan, A. Bramati, and M. Pinard, Phys. Rev. A **71**, 043801 (2005).
- [34] A. Lezama, S. Barreiro, A. Lipsich, and A. M. Akulshin, Phys. Rev. A **61**, 013801 (1999).
- [35] L. Vernac, M. Pinard, V. Josse, and E. Giacobino, Eur. Phys. J. D **18**, 129 (2002).
- [36] A. Dantan and M. Pinard, Phys. Rev. A **69**, 043810 (2004).
- [37] M. Sargent III, M. O. Scully, and W. E. Lamb, Jr., *Laser Physics* (Addison-Wesley, London, 1974).
- [38] C. Cohen-Tannoudji, J. Dupont-Roc, and G. Grynberg, *Atom-Photon Interaction. Basic Process and Applications* (John Wiley & Sons, New York, 1992).
- [39] N. Korolkova, G. Leuchs, R. Loudon, T. C. Ralph, and C. Silberhorn, Phys. Rev. A **65**, 052306 (2002).
- [40] A. M. Akulshin, S. Barreiro, and A. Lezama, Phys. Rev. A **57**, 2996 (1998).
- [41] A. Lezama, S. Barreiro, and A. M. Akulshin, Phys. Rev. A **59**, 4732 (1999).
- [42] A. Lipsich, S. Barreiro, A. M. Akulshin, and A. Lezama, Phys. Rev. A **61**, 053803 (2000).
- [43] D. Grison, B. Lounis, C. Salomon, Y. Courtois, and G. Grynberg, Europhys. Lett. **15**, 149 (1991).